Investigation of Solid Fuel Conversion in the Chemical Looping Process

A Bachelors of Science Thesis
Prepared in Accordance to Requirements for
Graduation with Honors in Engineering
And
Graduation with Distinction in Chemical and Biomolecular Engineering

Written By: Dennis Wayne McOwen

The Ohio State University 2010

Honors Thesis Committee:

Dr. Liang-Shih Fan

Dr. Barbara E. Wyslouzil

Approved By:

_____

Advisor

Abstract

The high energy density and abundance of coal along with the sustainability of biomass make them favorable fuels for energy production. However, the combustion of carbon-based fuels inevitably results in the production of the greenhouse gas carbon dioxide (CO_2). To avert climate change and comply with likely future regulations for greenhouse gas emissions, the CO_2 byproduct must be efficiently captured. Unfortunately, existing carbon capture methods result in significant decreases in plant efficiency and significant increases in capital and operating costs. The Coal-Direct Chemical Looping (CDCL) is an energy conversion process for coal/biomass that can separate the CO_2 stream in-situ by utilizing iron oxide composite particles as oxygen carriers. Using this method, the iron oxide particles provide crucial oxygen to the coal instead of air, which is the key strategy to the process. The cycling of the iron oxide particles allows for efficient and total carbon capture, therefore ensuring the sustainability and economic viability of carbon-fueled power. Although biomass also produces CO_2 upon combustion, it also absorbs CO_2 as it is grown. Therefore, biomass can be utilized as a replacement for coal and further improve the sustainability of the process by making it carbon negative.

The objective of this study is to investigate the enhancement of char and iron particle conversion with CO_2, design a mechanism for particle transfer from

the reducer to the combustor, and perform a preliminary assessment of the potential of biomass in the CDCL process. The main obstacle for CDCL is the conversion of coal char because the reaction between the metal oxide and the char is a slow solid-solid reaction. CO_2 was found to help gasify the char and significantly increase the rate of reaction. In fact, in the experiments performed in this study, the addition of CO_2 increased the amount of char reacted twofold. Furthermore, mixtures between 50% and 70% metal oxide with char were found to increase the char conversion the most compared to other mixtures. These mixtures increased the amount of char reacted 2-5 times, depending on the type of coal used. Ease of coal fluidization was found to be independent of the amount of metal oxide particles; however addition of 80-100% by mass of an inert particle was required in order to fluidize the biomass. A cold model of the reactor was constructed in order to study the gas-solid hydrodynamics and to design the most controllable method of handling solid fuels and oxygen carriers in the system. A design with high resistance and constant flow was selected based on experiments performed on the cold model. The results obtained by this study prove the capabilities of the CDCL process and will allow it to continue towards the scale up to a sub-pilot demonstration.

Dedicated to my brother David

“Force your dreams in reality.”

- E.T.M.

Acknowledgements

First and foremost I would like to thank Dr. Liang-Shih Fan for providing me the extraordinary opportunity to work in the chemical looping group. His motivation and enthusiasm for his field encouraged me to pursue an honors thesis. The experience I have gained in his lab I am sure will prove invaluable to my career. I am fortunate to have had Dr. Fan as an advisor and instructor as he has had a significant impact on my life and career.

Hyung Rae Kim has been an outstanding mentor to me and I could not have completed this work without him. I would like to thank Rae for the patience and thoughtful advice he has given throughout my time in the Fan Club. He has given me much practical experience and taught me many things about work in the lab and in graduate school. Rae's guidance and influence has been key to my education and I will not forget his support.

My appreciation goes to all members of Fan Club for showing me the ropes and lending me their support. The group was incredibly receptive and welcoming, helping to make my undergraduate research experience an exceptional one. I am grateful also to my friend Sean Lee for his advice, thoughtful discussions, and help in the lab. Thanks also goes to Adam Brandt for helping me to complete experiments when time was tight and to Emily Smith for her priceless aid, advice, and overall support.

I have Eric McChesney to thank for his everlasting friendship and commitment to perfection. He has infused in me a dedication to nothing less than great by my own standards and provided me with the will to continue in the hardest times. Zaia Thombre has a passion for life made of fire and has kindled parallel spirits inside me that make me who I am. The effect of my friend Glenn Rentner on me cannot be overlooked as he has given me his undying friendship and understanding as well as his unique perspective on all aspects of life.

I will never forget or take for granted the motivation my parents instilled in me as I grew up. It has taken me to great places and produced a great work ethic in me. My mother's late night encouragement and motivation along with my father's unwavering confidence in me has kept me going all through my undergraduate career. I love my parents and am forever indebted to them. I also acknowledge my brother, for I know he will always be there for me, and I for him. He will not settle for anything less than the best life and for that, I have the utmost respect for him.

Contents

List of Figures

List of Tables

List of Equations

Introduction

Background

Today it is well–known that climate change is a serious and threatening issue. The vast majority of scientists today have come to this conclusion through objective and thorough research. The main example is the results of a report by the Intergovernmental Panel on Climate Change (IPCC) which is an international scientific body set up by the United Nations Environment Programme and the World Meteorological Organization that reviews recent scientific research and observations to provide the public with a better understanding of what is happening in the global environment. In its fourth assessment (AR4) (1) released in 2007, the IPCC reported that the global average temperature increased by 0.74°C between 1906 and 2005. Though this temperature change may seem trivial considering that regional temperature fluctuations are of much larger magnitude than 0.74˚C, the average global temperature during the last ice age was only 5.6˚C different than today (2). It was also found that 11 of the 12 warmest years on record were from 1995 to 2006 giving evidence to the conclusion that the warming has increased in later years. Furthermore, the IPCC reported that the extension of sea ice has decreased and more and more is lost each year. Concurrently, sea levels have risen in the 20th century, and have been rising more rapidly in recent years as well. In March of 2010, a review of 110 research papers by the UK Met Office titled *Detection and Attribution of Climate Change: a Regional Perspective* (DACC) was published (3). The DACC report updates the findings of AR4 with research from 2007 to 2010 and reinforces the IPCC observations and conclusions concerning climate change in the world.

The debate is no longer whether climate change is real, but what actions need to be taken in order protect the world's natural resources and thus the global environment. In order to be able to make these decisions and take necessary action, the causes of climate change must be well understood. The IPCC AR4 reported that anthropogenic sources of greenhouse gas (GHG) emissions were "very likely" the cause of the rise in global average temperature on all continents except Antarctica. The DACC report further supports this IPCC conclusion and augments it by attributing Antarctic temperature changes to human activity, which the IPCC could not do in 2007 due to unavailability of data (3). The vast majority of other independent reports are in agreement with the findings that humans are in fact a major contributing cause of climate change.

Since the industrial revolution, human activity has required more energy consumption each year. As is evident in Figure 1 below, U.S. energy consumption has tripled since 1950 and will continue to rise. According to data from the U.S. Census Bureau, the U.S. population has doubled since 1950, indicating that each individual American is using more energy today than their 1950 counterpart. This comes as no surprise given the technological advancements made within the latter portion of the 20th century.

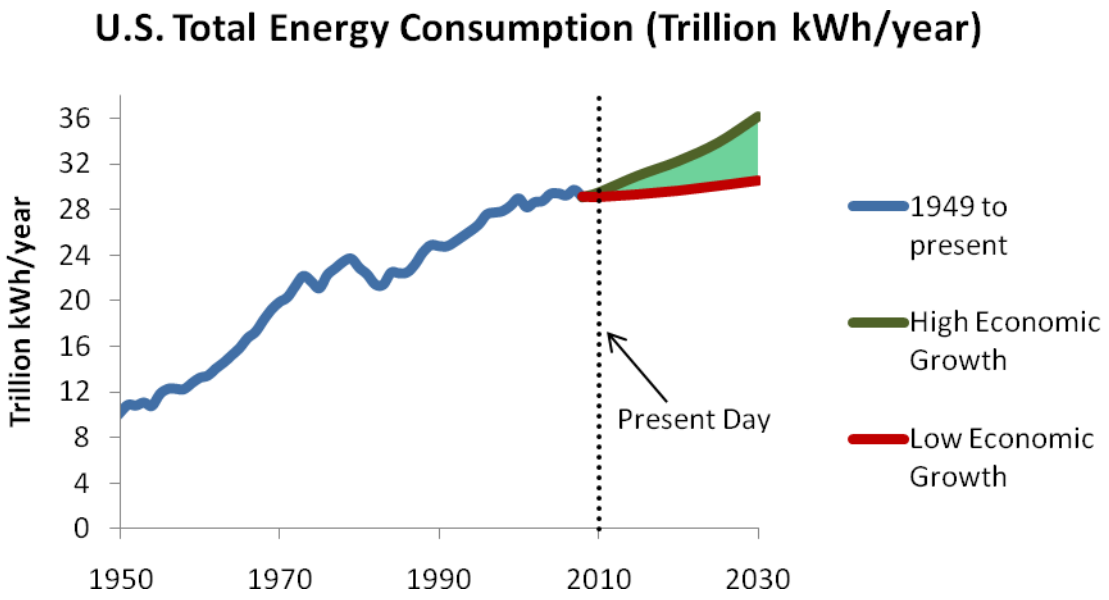

Figure 1: Total Energy Consumption of the United States each year since 1949 with projections to 2030, in trillions of kilowatt-hours (kWh). Data obtained from the U.S. Energy Information Administration (EIA) (4)

In order to meet the ever increasing energy demands, the usage and demand for fuel has increased accordingly. The consumption of major types of nonrenewable and renewable sources of energy since 1950 is shown in Figure 2 below. Fossil fuels are mainly coal, petroleum, and natural gas; renewable sources include wind, geothermal, and solar energy. Fossil fuels have seen major growth and are the most widely used source to meet the global energy demand, while renewable and nuclear electric power have remained stagnant. Fossil fuels have historically been much easier and simpler to find and use because they have been abundant and have high energy densities. Renewables typically require more complex technology and are more restricted by regional differences, such as the availability of wind or proximity to powerful water

flows. Nuclear energy requires heavy capital investment and an extensive permit process, both of which have contributed to stalling its growth.

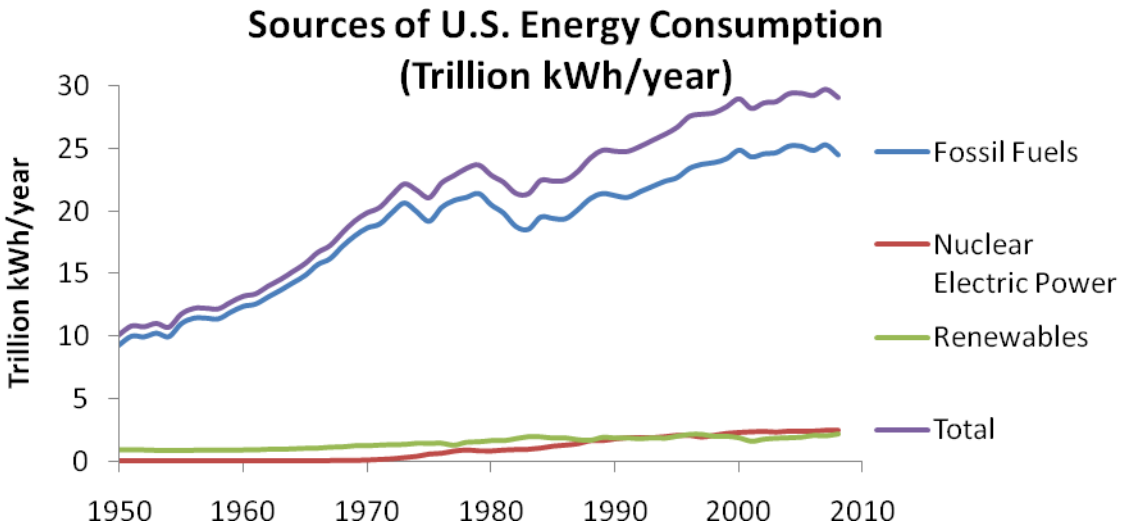

Figure 2: Sources of U.S. Energy Consumption from 1948-2008 in trillions of kWh. Data obtained from EIA (4).

The increase in energy demand and the subsequent rise in fossil fuels consumption has been a major cause of the increase in CO_2 emissions that is shown in Figure 3 below. The consumption of fossil fuels produces CO_2, which is an important GHG. CO_2 is naturally present in the atmosphere, coming from sources such as respiration of animals and decomposition of plant materials and animal life. The combustion of fossil fuels also inevitably produces CO_2. While plant life is capable of acting as a carbon sink, it cannot counter the quantity released by human activity. This imbalance has resulted in the increase in atmospheric CO_2 concentration by 35% since 1750 (5). In the past 650,000 years atmospheric carbon dioxide concentrations have never been as high as they are now (2).

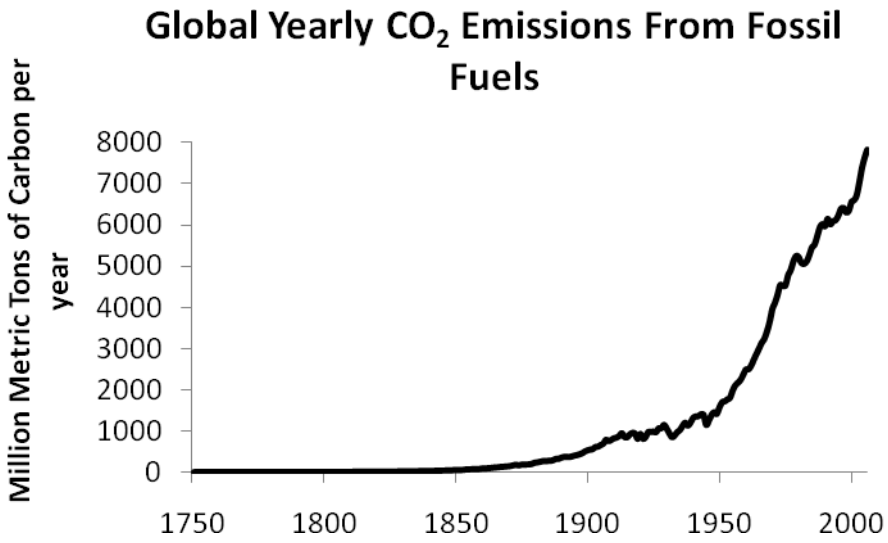

Figure 3: Global annual anthropogenic emissions of carbon dioxide. Data obtained from Carbon Dioxide Information Analysis Center (6).

Current Electricity Production

As of 2008, the US is responsible for nearly 20% of the CO_2 released globally, making it number two in overall CO_2 emissions (7). Of this, electricity generation is the most carbon-intense sector, accounting for 44% of all US CO_2 emissions (8). Globally, electricity is the main contributor to CO_2 as well. Electricity is produced mainly by fossil fuels, hydroelectric dams, and nuclear power. World electricity production by source is presented in Figure 4 below. Two thirds of the world's electricity is produced by fossil fuels, which is a main contributor to the massive amounts of CO_2 emissions depicted in Figure 3 above. Furthermore, future projections by the EIA indicate that while global energy demand will increase twofold by 2030, the percent contribution of each generation source will remain the same, indicated in Figure 5 below. Most importantly, the proportion used by coal, the most widely used source of energy for electricity

generation, will remain constant at just over 40%. The potential to reduce US and global CO_2 emissions by finding a new way to produce electricity with coal is therefore tremendous.

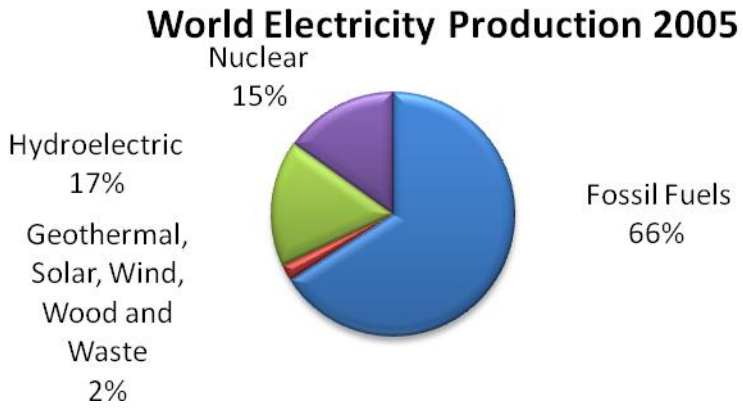

Figure 4: 2005 World Electricity Consumption by Source. (9) EIA

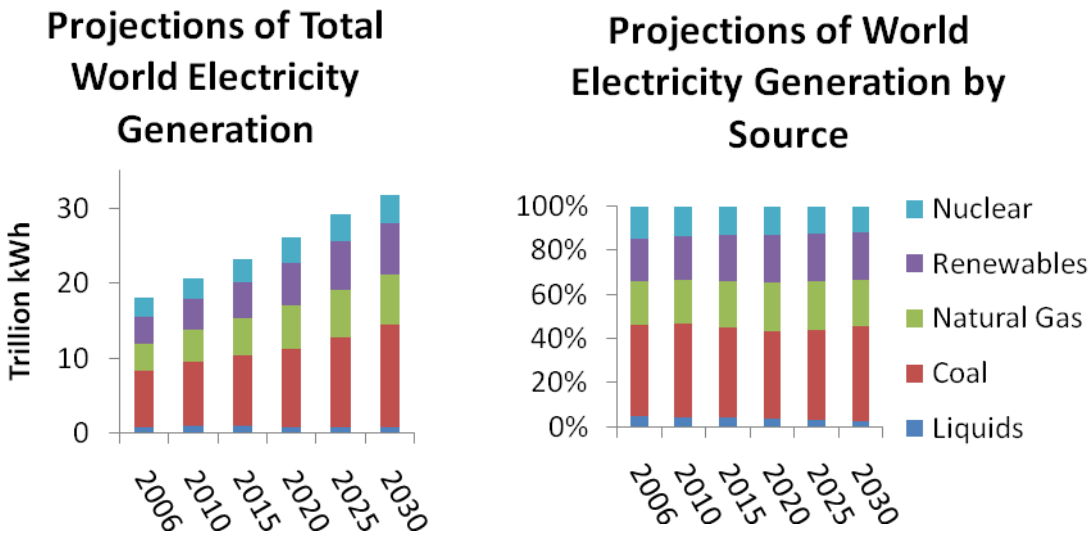

Figure 5: Projected global trend in electricity production. Total Generation by energy source is shown on the left and energy source by percent is shown on the right (10).

The main method used to convert coal to electricity is Pulverized Coal Combustion (PCC). In PCC the coal is milled to a very fine powder and burned at high temperature with air. Pulverizing the coal increases the surface area of the fuel so it may burn more quickly. The heat is used to produce high pressure steam which is then run through a turbine to produce electricity. Coal has several toxic pollutants like mercury and sulfur which are difficult to remove before combustion. Therefore, the flue gases are typically scrubbed for sulfur and mercury compounds before they are released. However, all of the carbon dioxide is released to the atmosphere. Another method called Integrated Gasification Combined Cycle (IGCC) has recently come into the commercial spectrum. IGCC gasifies the coal and separates the pollutants before combustion and has the potential to increase plant efficiency.

It is likely that in the future CO_2 emissions will be regulated and coal plants will need to find a way to reduce their emissions (11). One way to meet this goal is to capture and sequester the CO_2. Carbon sequestration requires high purity CO_2 (12). Since the coal fuel is burned with air in the IGCC and PCC designs, the resulting flue gases are dilute in CO_2, about 10-15% by volume (13) (14). Therefore, capturing the CO_2 from the flue gases of either type of plant design requires purification. Unfortunately, the most common methods of CO_2 separation, like MEA absorption, have a large energy penalty and are not cost-effective (15) (16). It has been predicted that to capture 85% of a PC plant's CO_2 emissions, a 30% energy penalty would be associated, doubling the cost of the electricity generated to 9.4¢/kWh. For an IGCC plant, the energy penalty is estimated to be 23%, and also increasing the cost to 9.4¢/kWh (16). The CDCL process converts coal using an oxygen carrying metal oxide particle instead of contacting the coal with air.

Therefore, the gaseous product is not diluted, resulting in a high purity CO_2 stream that is sequestration ready without the additional energy penalty of PCC or IGCC designs.

Coal Direct Chemical Looping

A novel technology termed Coal Direct Chemical Looping (CDCL) is the emphasis of this study. The promise of CDCL is that it extracts the energy in carbonaceous fuels like coal and biomass to produce electricity while capturing 100% of the carbon dioxide emissions without the large energy cost of traditional capture methods. CDCL does not combust coal with air. Instead, a metal oxide is used as an oxygen carrier to oxidize the fuel, meaning that the coal never comes into contact with air and the CO_2 product is retrieved in high purity. The energy-intensive separation step of conventional coal plants is thus avoided, maintaining plant efficiency and effectiveness.

A diagram of the process is shown in Figure 6 below. There are two main sections of the process: the reducer and the combustion train. In the reducer, pellets of iron (III) oxide (Fe_2O_3) are introduced from the top section while pulverized coal is injected in the middle. Fe_2O_3 was chosen over other metal oxides because it has been proven to have high recyclability and oxygen carrying capacity. The reducer is maintained above 800˚C, within the temperature range that the reduction of Fe_2O_3 is effectively active (17). The volatiles and carbon in the coal can be oxidized by the oxygen in the Fe_2O_3. However, while volatile conversion is relatively fast, the carbon-Fe_2O_3 interaction is a solid-solid reaction so the kinetics are too slow (18). Enhancing the conversion of the solid carbon, or char, is the main focus of this study. The method employed is to inject CO_2 from the bottom of the reactor to partially oxidize the coal via Equations 1 and 2. The gaseous CO

can then react with the Fe_2O_3 much faster to produce reduced Fe, FeO, and CO_2, as shown in Equations 3 and 4.

Equation 1: $Fe_2O_3 + C \rightarrow FeO + Fe + CO_2$
Equation 2: $CO2 + C \rightarrow 2\ CO$
Equation 3: $Fe_2O_3 + CO \rightarrow CO_2 + 2FeO$
Equation 4: $FeO + CO \rightarrow CO_2 + Fe$

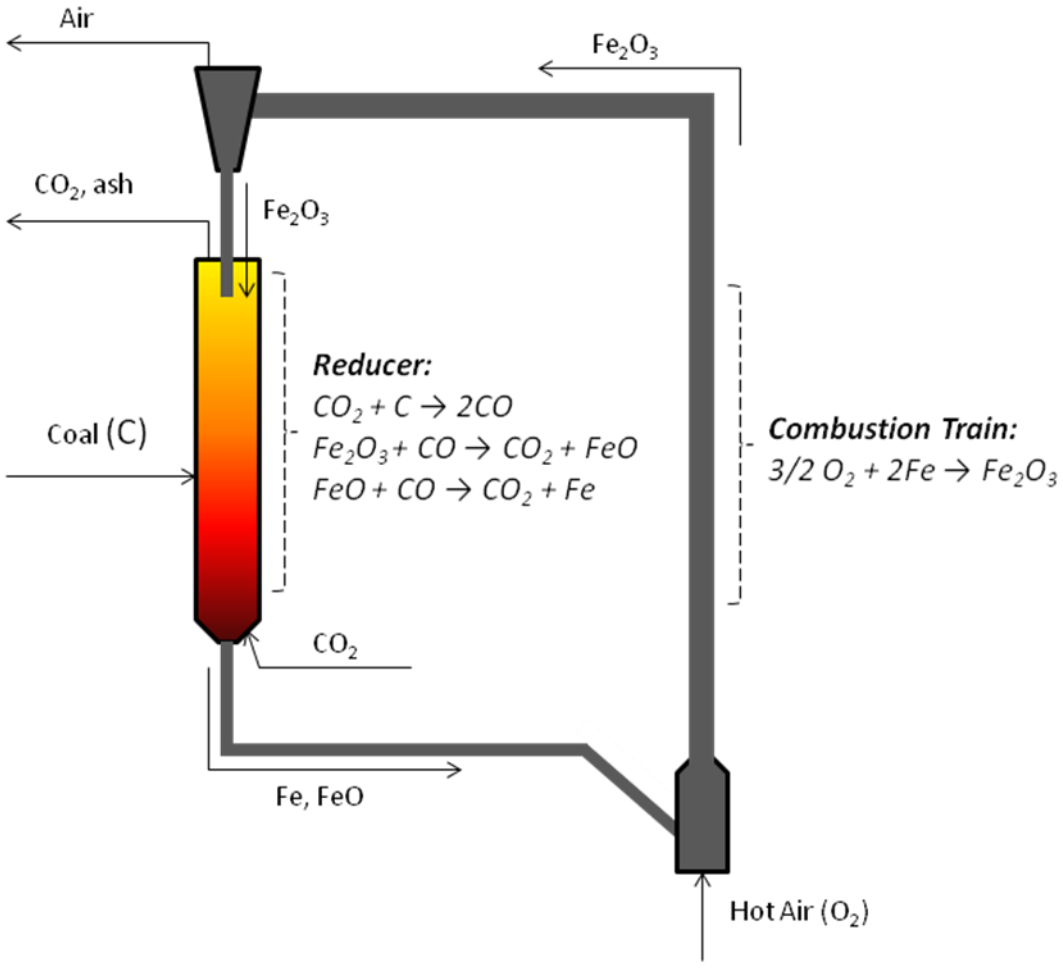

Figure 6: CDCL Process Diagram

The iron pellets are packed into the reactor from the top and travel slowly down the reactor in a moving bed. The CO_2 is injected at the bottom of the reactor to fluidize the pulverized coal to help gasify it faster. If the iron oxide were fluidized with the coal, the iron would become oxidized by the CO_2 instead of being reduced by CO, meaning less energy can be recovered in the combustion train. Therefore, the coal travels up the reactor with the reactive gas, countercurrent to the iron particles to ensure maximum fuel oxidation and iron reduction. Ash is entrained out of the top of the reactor.

The second section is the combustion train. Once the iron is reduced and exits the bottom of the reducer, it moves to the combustion train where hot air is used to entrain the particles up and back to the top of the reducer, completing the loop. In the process, the iron reacts with the oxygen in the air via Equation 6. Since the reaction is highly exothermic, it is used to produce steam to drive turbines and generate electricity.

Equation 5: $FeO + O_2 \rightarrow Fe_2O_3$
Equation 6: $4Fe + 3O_2 \rightarrow 2Fe_2O_3$

At the top of the reducer is a cyclone which allows the hot air to vent out of the top but ensures the iron particles return to the reducer.

There are several advantages to the CDCL design over the IGCC and PCC designs. Since air never contacts the fuel, the CO_2 that exits the top of the reducer is high purity and ready for sequestration without additional separation processes. The elimination of CO_2 separation steps makes carbon capture more economical and the transition to carbon neutral electricity generation easier. Furthermore, CDCL is expected to be retrofit to current PCC plants, which account for the majority of the coal fired power plants in the world (19) (20) . The ability to retrofit saves money and resources,

while also addressing the issue of climate change and GHG emissions faster than building a new plant. Lastly, CDCL has the ability to use biomass since it is a carbon-based fuel. Utilizing biomass would mean electricity generation that is a carbon sink, since the CO_2 is captured and sequestered.

The focus of this study is to understand the reactions in the reducer and explore preliminary reactor configurations. Some key questions must be answered for CDCL to be a replacement for traditional plant designs with CO_2 capture. First, the kinetics of the coal char gasification by CO_2 in the presence of the oxygen carrier iron oxide are not well understood in the conditions of the reducer. Initial testing revealed the kinetics of char conversion were too slow to be economical, so the effects of the presence of iron oxide and CO_2 were explored to determine potential methods for increasing the gasification rate. The char gasification study is a key element to the performance of the CDCL design.

Another method to increase char conversion is fluidize the char. However, to fluidize the iron particles would mean decreased particle reduction, and a loss of recoverable energy. The countercurrent moving bed of iron particles and fluidized bed of char is designed to increase char conversion and reaction rate without sacrificing particle conversion. However, this design presents unique reactor design challenges. In gas-solid fluidization, the lowest gas velocity that fluidizes the solid is known as the minimum fluidization velocity (U_{mf}). It was unknown whether the amount of fuel relative the iron particles in the reducer (F:P ratio) would affect the U_{mf}, and therefore the total gas velocity entering the reducer. A small fluidizer was setup to examine the effect of the F:P ratio on the U_{mf} using both coal and biomass.

To be able to utilize biomass as a replacement fuel for coal, many questions must be answered. One known issue is that biomass can be difficult to fluidize due to agglomeration. Larger grain biomass sticks to itself making it difficult to break apart and fluidize. It also has a high void fraction which maintains a low pressure differential in the fluidizer, requiring a higher U_{mf}. Once the gas velocity is high enough, the smaller grain biomass forms one continuous structure inside the reducer with several large holes, allowing the gas to escape and preventing fluidization. In early studies, increasing the gas velocity did not prevent structure formation. Addition of an inert particle to the biomass inside the fluidizer has the possibility of being able to prevent biomass structure, decrease the void fraction, and break up bonds between biomass grains (21). As a preliminary assessment of the feasibility of biomass to be used in the CDCL process, its ability to be fluidized was studied under different conditions in the fluidizer.

Another important factor in the reactor design is the mechanism to transfer the reduced iron particles from the moving bed in the reducer to the combustion train to be oxidized and generate the heat that is key to producing electricity. The flow of particles to the combustion train needs to be low but easily controllable and adjustable so as to maintain the correct particle residence time in the reducer and not overfill the combustion train. A scale cold model of the CDCL process was built to explore different options for the particle transfer design.

Experimental Methods

Char Gasification

In order to determine the dependence of char gasification (Equations 1 and 2) on the oxygen carrier, the kinetics of char gasification were studied in a fixed bed reactor and a thermogravimetric analyzer (TGA). Different mixtures of coal and Fe_2O_3 powder were created and analyzed in the TGA to give a qualitative understanding of the presence of the oxygen carrier. Several configurations of coal and Fe_2O_3 particles were studied in the fixed bed to better simulate the reducer and understand the effect of the position of the oxygen carrier on char oxidation. Furthermore, it was hypothesized that different types of coal would have different dependencies on the oxygen carrier. Various different types of coal were examined to observe their differences. A summary of the performed experiments is presented in Table 1 below.

The fixed bed was a 36" glass pipe with a 5/8" inner diameter placed inside a heater. The fixed bed experiments were performed three ways: char with no oxygen carrier (configuration A), char mixed with the oxygen carrier (configuration B), and char separated and packed on top of the oxygen carrier (configuration C). These configurations are shown in Figure 7 below. First, chars of lignite, anthracite, and sub-bituminous coals were prepared by heating the raw coal in a fixed bed reactor with 100% nitrogen (N_2) flow at 900°C for about four hours. Configuration A corresponds to the charring process. This procedure removes moisture as well as any volatiles in the raw coal that would react with the Fe_2O_3.

Table 1: Summary of experiments in fixed bed reactor and TGA. Configurations can be found in Figure 7 on page 15 below. P = Iron Particles, Ch = Char

Run #	Char Type	Configuration	F:P Ratio	Fixed Bed Environment	TGA Environment
1	Lignite	N/A	100:0	N/A	100% N2
2	Sub-bituminous	N/A	100:0	N/A	100% N2
3	Lignite	C	Excess	5% CO2	P:Air, Ch:Air
4	Lignite	C	Excess	100% N2	P:Air, Ch:Air
5	Anthracite	C	Excess	5% CO2	P:Air
6	Anthracite	C	Excess	100% N2	P:Air
7	Sub-bituminous	C	Excess	5% CO2	P:Air
8	Sub-bituminous	C	Excess	100% N2	P:Air
9	Lignite	N/A	10:90	N/A	100% He
10	Lignite	N/A	30:70	N/A	100% He
11	Lignite	N/A	50:50	N/A	100% He
12	Lignite	N/A	70:30	N/A	100% He
13	Lignite	N/A	90:10	N/A	100% He
14	Lignite	N/A	100:0	N/A	100% He
15	Lignite	N/A	70:30	N/A	5% CO2
16	Lignite	B	100:0	22.5% CO2	N/A
17	Lignite	B	70:30	22.5% CO2	N/A
18	Sub-bituminous	N/A	10:90	N/A	100% He
19	Sub-bituminous	N/A	30:70	N/A	100% He
20	Sub-bituminous	N/A	50:50	N/A	100% He
21	Sub-bituminous	N/A	70:30	N/A	100% He
22	Sub-bituminous	N/A	90:10	N/A	100% He
23	Sub-bituminous	N/A	100:0	N/A	100% He
24	Sub-bituminous	N/A	50:50	N/A	5% CO2
25	Sub-bituminous	B	100:0	22.5% CO2	N/A
26	Sub-bituminous	B	50:50	22.5% CO2	N/A

Mixtures of 0%, 10%, 30%, 50%, 70%, and 90% Fe_2O_3 powder were created with the lignite and sub-bituminous chars. The mixtures were run in the TGA at 900˚C for 70 minutes in an inert environment of Helium (He) to compare the changes in mass due to the presence of differing amounts of Fe_2O_3. The products of the best mixture were run in the TGA again with 5% CO_2. The mass change for these TGA experiments allows for the

determination of the extent of the solid-solid oxidation reaction of the char by the oxygen carrier Fe_2O_3 (Equation 1), the oxidation of the char by CO_2 when it is present (Equation 2), and the reduction of the Fe_2O_3 (Equations 3 and 4). The mixtures which resulted in the most mass lost in TGA were then recreated using the Fe_2O_3 pellets and run in the fixed bed at 900˚C for 90 minutes with 22.5% CO_2 and balance N_2. This experiment corresponds to configuration B in Figure 7 below. The outlet gases were analyzed as the exited they fixed bed by gas chromatography. This process was repeated with 100% char and no Fe_2O_3 particles in Configuration A to establish the effect of the Fe_2O_3 on the rate and extent of the char gasification.

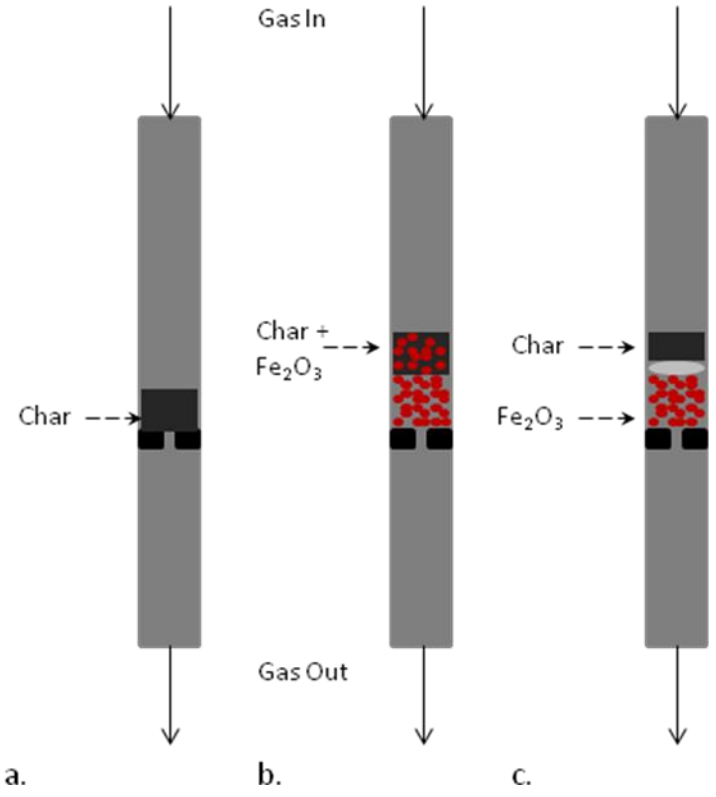

Figure 1: Fixed bed configurations A, B, and C. Gas Inlets were 100% N_2, and 5% CO_2, balance N_2.

The fixed bed was then packed with about 10g of Fe_2O_3 particles and 1-2g of char in configuration C. The fixed bed was heated and held at ~120-160°C for 20-30 minutes to remove any accumulated moisture after the charring process, and then held at 900°C for at least four hours. By comparing configuration A to B and C, the relative contributions of the char solid-solid reaction with Fe_2O_3 and char gasification to produce reducing gases can be determined.

Configuration C was run two different ways: once with 5% CO_2 and balance N_2 at 30mL/min and once in an inert environment of pure N_2 at the same flow rate. To determine the effect of the presence of CO_2, the reduced iron particles and partially oxidized char from the fixed bed were oxidized in the TGA. Samples of either char or iron particles were held in the TGA at 20˚C for 10 minutes to establish an initial mass, heated and held at 900˚C for 15 minutes, then cooled back to 20˚C. Air was used as the oxidizing gas at 100 mL/min with 50 mL/min N_2.

Since the energy in the CDCL process will be recovered by oxidizing the iron particles, a more direct measurement of useable energy from the char oxidation in the reducer is to compare the oxidation of iron particles after they have been reduced in the fixed bed. The iron particles were first homogenized to ensure a representative sample was used in the TGA. The oxidation would oxidize all iron back to Fe_2O_3. Since the Fe_2O_3 particles would be reduced in the fixed bed reaction by the CO produced by char gasification, oxidation of the particles in the TGA would increase the mass. The increase in mass is expected to be less for experiments run in the inert environment. No CO can be formed by Equation 2 if no CO_2 is present, thus lowering the amount of reducing gases

available to the Fe_2O_3. In this case, less Fe_2O_3 is reduced, resulting in less mass gained by oxidation in the TGA.

Similarly, char run in an inert fixed bed environment should have a greater mass loss in the TGA than char run in the 5% CO_2 experiments. An inert environment should result in less char being oxidized in the fixed bed. Oxidation in the TGA would consume the remaining char leaving only ash, but less char would be available if some char has reacted by Equation 2 in the fixed bed. To understand the extent of char gasification, it is first necessary to be able to correlate the mass gained by the iron particles and the mass lost by the char in the TGA to the amount of char that is gasified by Equation 2. For the iron particles, it is assumed that iron is completely oxidized and all mass gained in the TGA is oxygen. The percent mass gained is equivalent to the percent mass lost by reduction of the iron particles in the fixed bed due to the reducing gas CO (Equations 3 and 4). The CO is produced by Equation 2 with a 1:1 ratio to the amount of carbon gasified. Therefore, the relation between mass gained by the iron particles in the TGA and percent of char gasified (G) is given by Equation 7, below,

Equation 7:
$$G = \frac{12\left(x - \frac{x}{1+\frac{y}{100}}\right)}{16m}$$

where y is the percent mass gained by iron in the TGA, x is the original mass of iron in the fixed bed (g), 12 and 16 are the molecular weights of carbon and oxygen, respectively, and m is the original mass of char in the fixed bed (g). A possible error in this equality could be result from volatiles reacting with the Fe_2O_3 due to incomplete charring.

Fluidization

The amount of pulverized coal or biomass inside the reactor relative to the amount of packed iron particles is a crucial parameter due to its effect on the kinetics of the reactions. However, the F:P ratio could also affect the gas velocity required for fluidization of the coal or biomass fuel. Fluidization is important because, like CO_2, it helps to increase char conversion. To determine the optimum F:P ratio for fluidization, biomass and coal were fluidized on a fixed bed of iron particles in a 2' long, 2" inner diameter pipe, with gas injection from the bottom. The pressure differential (ΔP) was measured from the bottom to the top of the fluidizer and observations regarding the state of the bed were recorded. A diagram of the fluidizer is shown in Figure 8 below.

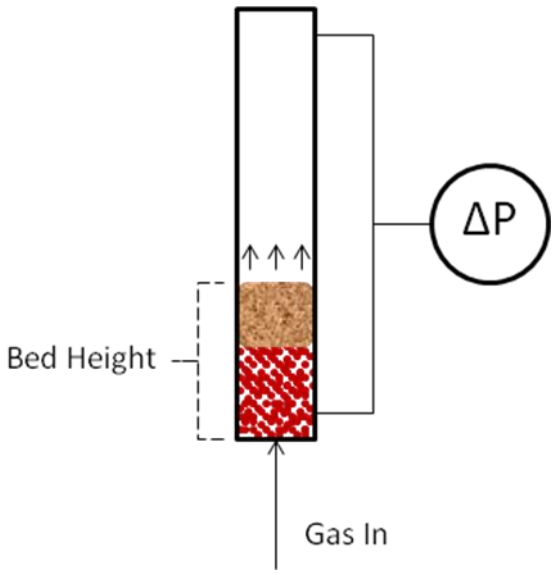

Figure 8: Diagram of fluidizer used to fluidize sand to simulate coal, as well as wood biomass.

First, about 100g of Fe_2O_3 particles were packed into the fluidizer. To simulate pulverized coal, fine grain sand was used. Then, the gas velocity was slowly increased using a mass controller and the ΔP and bed height were read at every 1 L/min. This process was repeated 5 times, each changing the amount of sand in the fluidizer to give F:P ratios of 1:0, 1:1, 2:1, 3:1, and 1:2. When a solid is fluidized, the ΔP will drop sharply and the gas velocity at which this occurs is called the minimum fluidization velocity (U_{mf}). When only one size solid is present, the ΔP will remain constant after fluidization. However, since the iron particles are much larger than the sand, they do not fluidize when the sand does. The slow increase in pressure drop after the sand fluidization is caused by the iron particles. The pressure drop will continue to increase until the iron particles are fluidized. At this point, the gas velocity would be so high that the sand would be entrained out of the fluidizer.

To test the fluidization of biomass, the same procedure was followed as for coal. Two different sizes of wood grain were used and it was soon found that it was quite difficult to fluidize both of them, as predicted by the literature (21). The larger grain wood tends to agglomerate and resist fluidization. It also has a high void fraction which keeps the pressure differential low. The smaller grain wood forms structure and holes where gas could escape, preventing fluidization. The gas velocity required to fluidize both grain sizes of wood was far too high to be economical and at these points, fluidization was still unstable. Other studies have achieved some success by adding an inert material into the biomass to prevent agglomeration. However the use of correlations to predict U_{mf} or amount of inert to add has been inaccurate due to the complex and varying properties of biomass (21). Therefore the U_{mf} was determined by experiment.

The type of inert particle to use depends on several key factors. It needs to be able to withstand the high temperatures of the reducer, prevent agglomeration and structure of the wood grains, and fluidize with the wood in one phase. The particle FCC could satisfy all of these conditions. Different amounts of FCC were added based on percentage of biomass weight. The bed height and pressure drop across the fluidizer were recorded as the gas velocity was increased. Mixtures of 0%-150% FCC by mass of wood grains were tested in the fluidizer. Observations were also recorded indicating bubble formation, partial fluidization, full and stable fluidization, and entrainment.

Cold Model: Particle Flow

In order to study particle flows inside a sub-pilot scale 25 kW_{th} reactor and understand the influence of certain reactor design parameters, a cold model was constructed. The model was constructed out of clear acrylic plastic so flow dynamics could be observed from the outside. A steel frame was used as a support structure and the final model was about 20 ft tall. The diameter of the reducer section was 5" while connections and the combustion train were 2" in diameter. To simulate the Fe_2O_3 particles, 3.5-4.0 mm diameter glass beads were packed in the cold model, and a Fluidized Catalytic Cracking (FCC) particle was injected to model the pulverized coal. Air was used as gas injection from the bottom of the reducer, to inject the FCC, and in the transition from the reducer to the combustion train.

One challenge of the reactor design was to be able to ensure a low, controllable, and steady flow rate of particles out of the bottom of the reducer to the combustion train. In order to find the best method of doing so, factors that could possibly affect the particle flow rate were determined. These criteria were smooth or sharp angle of the output pipe,

bottom or top air injection, size of restriction blade, and pipe diameter. A diagram of these properties is shown in Figure 8 below. Table 2 below summarizes the ten different combinations of the properties which were tested.

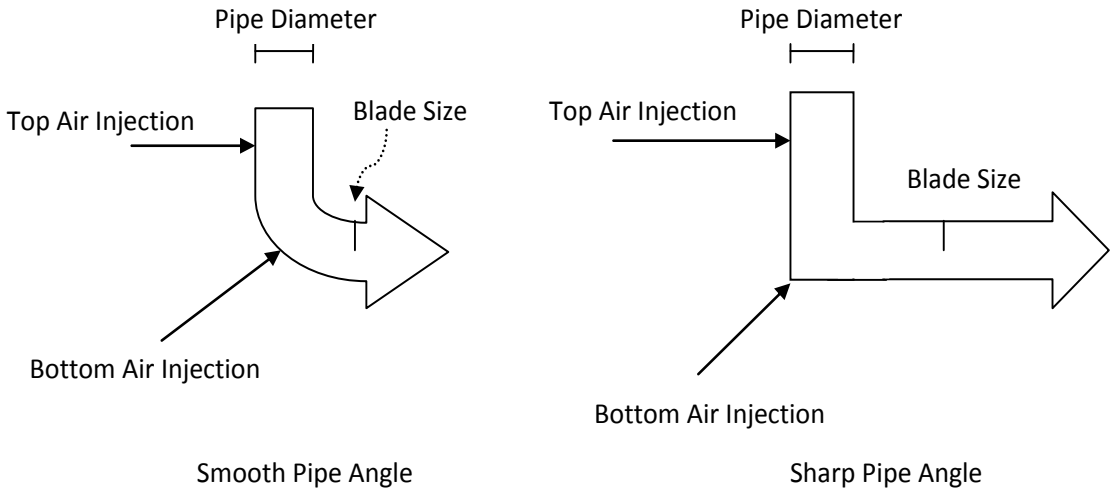

Figure 2: Diagram of possible reducer output design for particle outflow to combustion train

Table 1: Tested designs for particle outflow of reducer.

Model #	Pipe Size (in)	Angle Shape	Blade Enclosure	Air Injection
1	2	Sharp	1/3 Blade	Top Air
2	2	Smooth	1/3 Blade	Top Air
3	2	Sharp	1/3 Blade	Bottom Air
4	2	Smooth	1/3 Blade	Bottom Air
5	2	Smooth	1/2 Blade	Bottom Air
6	2	Smooth	1/2 Blade	Top Air
7	2	Sharp	1/2 Blade	Top Air
8	1.5	Sharp	NO	Bottom Air
9	1.5	Sharp	NO	Top Air
10	1.5	Sharp	1/3 Blade	Top Air

Each combination was tested three times and the output flow rate of the particle was measured by collecting the particles in a bucket as they came out for one minute. A smoother pipe angle was predicted to provide for less resistance while sharper would provide more resistance. Air injection would help to break up particle structure and prevent holdup, but it was unclear where to place the air injection. Therefore, two sites were chosen to be tested: bottom and top. The restriction blade would allow for control of particle flow while breaking up particle structure and preventing holdup as well. It was also expected that a larger pipe diameter would allow for a higher particle flow rate as well as require a higher air flow rate in the air injectors than the smaller pipe diameter.

Results and Discussion

Char Gasification

Before analysis of any experiments with coal char, it is imperative to have a blank to compare to. Runs 1 and 2 from Table 1 were 100% char samples run in an inert environment in the TGA. As seen in Figure 10 below there is a small amount of weight loss for each of the chars. The sub-bituminous char loses almost 8% of its mass. This represents accumulated moisture and some volatiles that remained after the charring process. In experiments that could be effected by this, chars were either heated and held between 100-200˚C to minimize the influence of moisture and volatiles on the results, or compared to the blank results.

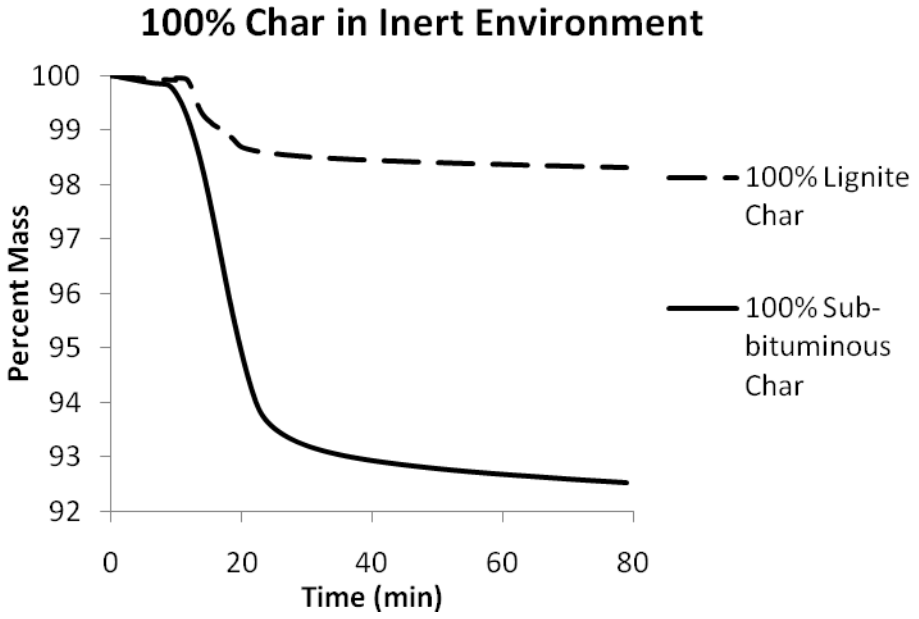

Figure 3: Demonstration of the mass lost by 100% char in He after charring process.

TGA analysis of the different F:P ratios in an inert environment at 900°C (runs 9-15 and 17-23) provided different results for lignite and sub-bituminous coal chars. As can be seen in Figure 11 below, the mixture of 70:30 lignite char to iron particles resulted in the most mass loss.

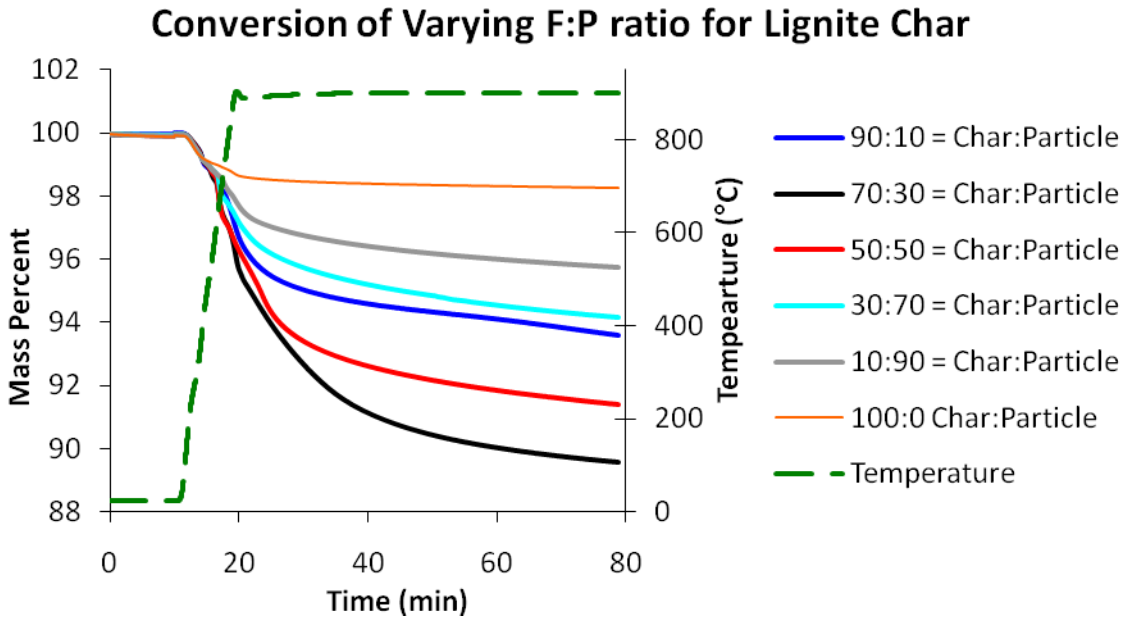

Figure 11: Effect of varying the amount of Fe_2O_3 mixed with the lignite char on char conversion in inert environment of He.

For the sub-bituminous char, 50:50 F:P was the best ratio. Since lignite is a low rank coal, it has less available carbon than sub-bituminous coal (22). Therefore a higher F:P ratio is needed to compensate and achieve the greatest extent of reaction. Lignite's greatest mass loss was 11% while for the sub-bituminous char it was 15%. The mass lost is both from char gasification and iron reduction. Since the sub-bituminous coal has more available carbon, more char can react which also means more iron will be reduced, both

of which contribute to the greater mass loss of sub-bituminous char over lignite char. Furthermore, for both lignite and sub-bituminous chars, the addition of iron oxide always resulted in more mass lost in the TGA, demonstrating the effectiveness of the oxygen carrier particle.

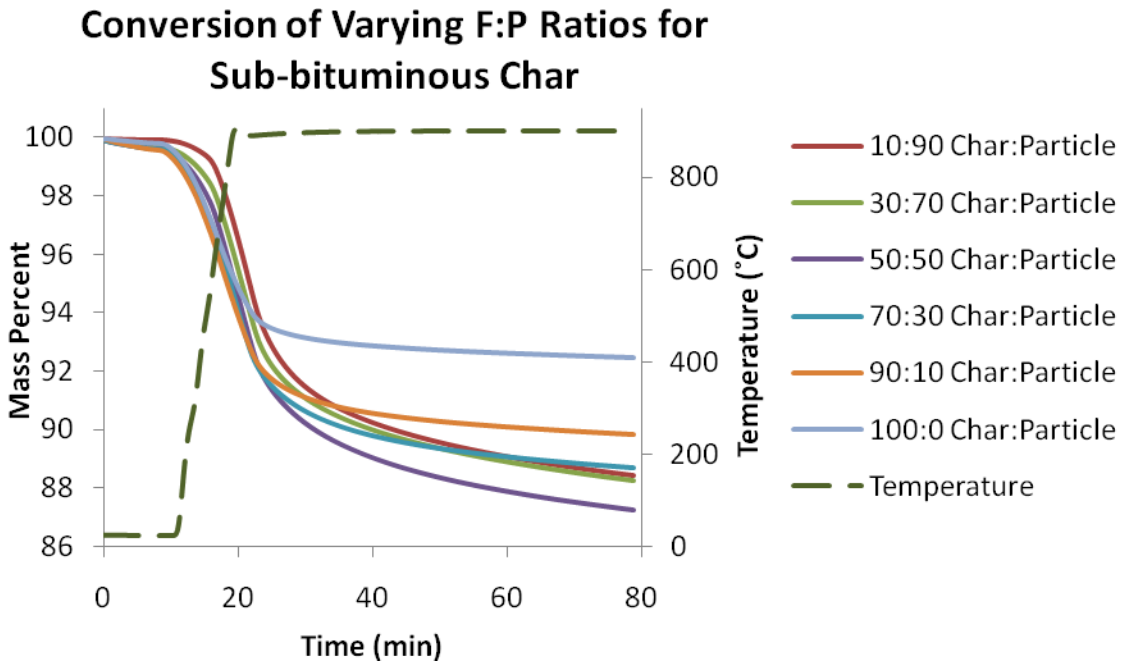

Figure 12: Effect of varying the amount of Fe_2O_3 mixed with the sub-bituminous char on char conversion in inert environment of He.

To gain a primary estimate of the effect of CO_2 on the extent of char consumption, lignite char which had been run in configuration C with and without CO_2 was oxidized with air in the TGA at 900°C (runs 3 and 4). The change in mass over time in the TGA is shown Figure 13 below. The remaining mass after oxidation is due to the ash content which cannot be combusted. The mass lost represents gasified carbon, as well as a small amount of accumulated moisture and remaining volatiles. The TGA analysis

shows that lignite char run in the fixed bed is oxidized 3.6% percent more with CO_2 present, proving that CO_2 enhances char gasification by Equation 2.

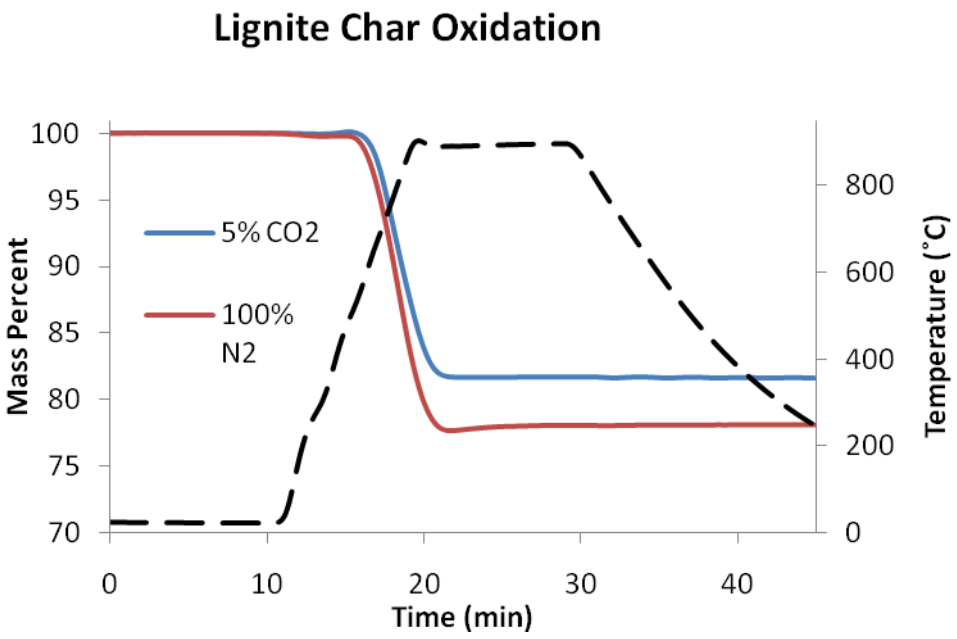

Figure 13: TGA oxidation with air of lignite chars which had been run in fixed bed configuration B with and without 5% CO_2 (runs 3 and 4).

Reaction of the best F:P ratios in both inert and CO_2 environments shows the effect of CO_2 on char gasification. The mixtures had previously been reacted in an inert environment of He in the TGA, so most of the change in mass can attributed to the CO_2 gasifier. The gasification-enhancing effect of CO_2 is clearly evident below, in Figure 14, which depicts results from runs 10, 15, 20, and 24. The mass loss was significantly higher for samples in a CO_2 environment; the sub-bituminous char had mass losses of 5% and 10% with N_2 and CO_2 respectively and the lignite had mass losses of 2% and 4%. The reduction of the iron oxide that was mixed with the char also contributed to the mass loss. The presence of the iron particle does not degrade the gasification effect of the CO_2 but

rather enhances it, thereby proving the application of Equations 2, 3 and 4 in the CDCL design.

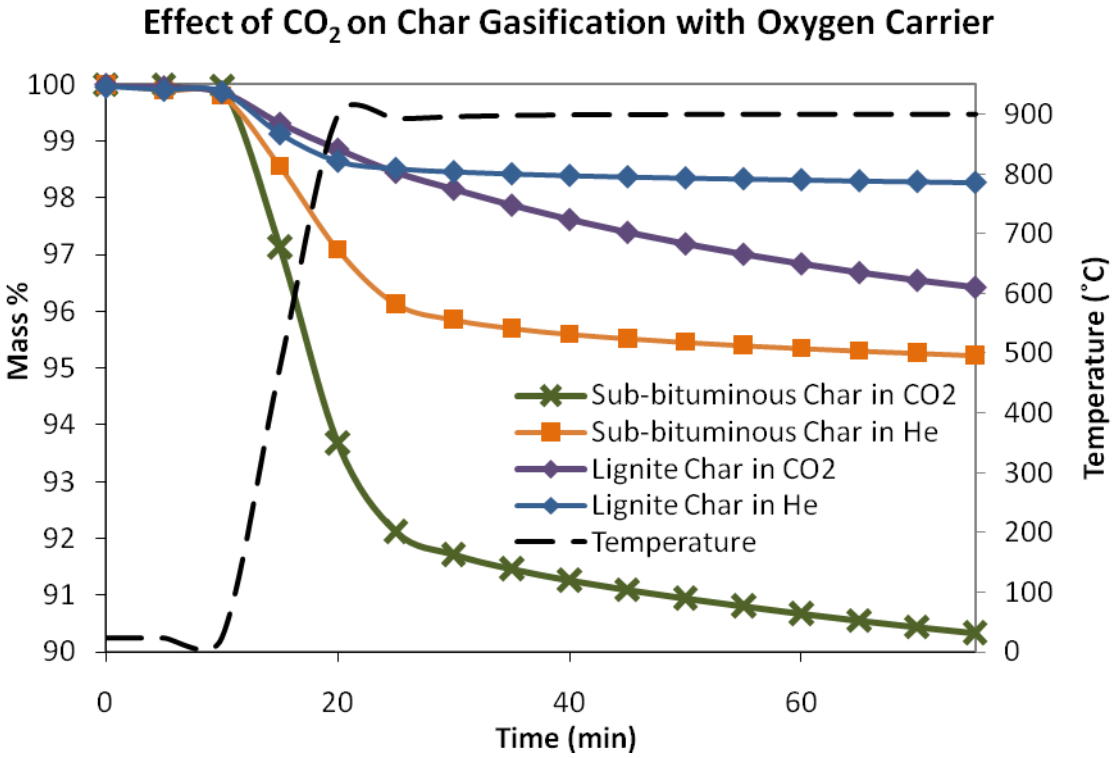

Figure 14: Demonstration of the effect of CO_2 on char gasification using the F:P ratios of 70:30 for lignite and 50:50 for sub-bituminous char.

Homogenized samples of the iron particles from each fixed bed experiment were analyzed in the TGA. Analyzing the iron particles as opposed to the char is a more accurate measurement of extractable energy because some of the CO from the gasified char may not react with the Fe_2O_3, representing a loss of available energy. In each case, the presence of CO_2 resulted 5-10 times higher reduction of the iron particles in the fixed bed compared to the inert environment. The results for lignite char are shown in Figure 15, below, and summary of results with each char is shown in Table 3, below. Graphical

results from the sub-bituminous and anthracite samples can be found in Appendix A. The ratio column displays the ratio of char reacted with CO2 to char reacted in an inert environment. Each ratio is much greater than 1, showing that CO_2 significantly increases the amount of char converted. The percentage of char reacted is higher for the sub-bituminous char than for anthracite or lignite. This corresponds to the higher mass lost by sub-bituminous char in the blank run compared to the lignite char. The sub-bituminous char was noted to be a much finer particle than the lignite or anthracite which may have made the carbon more available to reaction. It is also possible the sub-bituminous char was not charred completely. Nevertheless, CO_2 clearly increases the conversion of each type of char, further confirming the ability of CO_2 to enhance gasification.

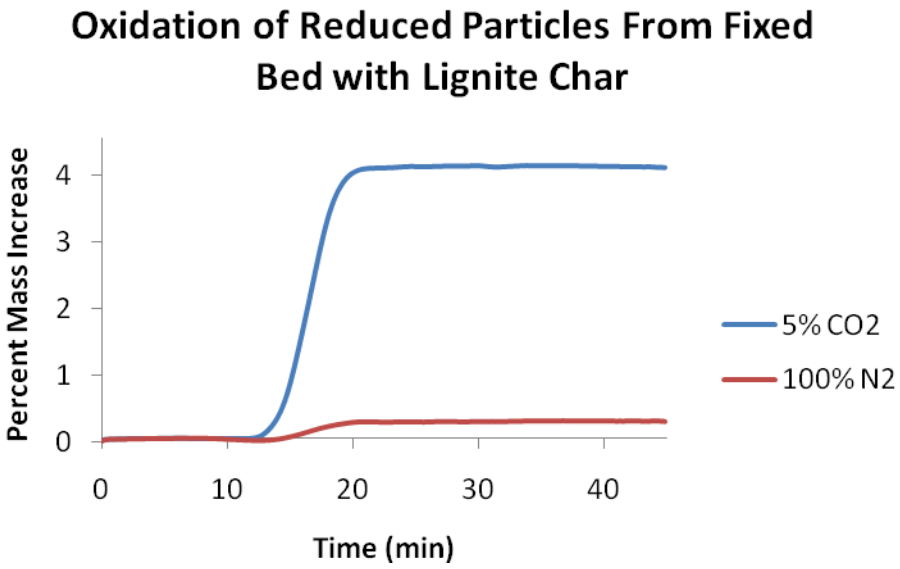

Figure 4: Oxidation of the iron particles from runs 3 and 4 which had been reduced by the char. Larger mass increase when CO2 is present indicates higher particle reduction and more char gasification.

Table 3: Comparison of iron particles from fixed bed experiments in configuration C (runs 3-8).

	With CO_2		Without CO_2		
Type of Char	% Mass Increase of Particle	% Char reacted	% Mass Increase of Particle	% Char reacted	Ratio
Lignite	4.1%	12.8%	0.3%	1.2%	11
Sub-bituminous	6.7%	37.5%	0.9%	7.7%	5
Anthracite	3.0%	11.2%	0.4%	1.8%	6

The analysis of the outlet gases of fixed bed configuration C provides a better understanding of the effect of Fe2O3 particles on the rate of gasification. The results of the lignite char experiments (runs 16-17) are shown in Figure 16, below, while the sub-bituminous results (runs 25-26) may be found in Appendix A. Without Fe_2O_3, the CO_2 concentration of the exit gases starts well below the inlet concentration representing the CO product from conversion of the CO_2 gasification of char in Equation 2. After 100 minutes, it is clear the reaction is not close to completion because outlet concentration is only 15% and increasing very slowly. In fact, there is little change in the outlet concentration of CO_2 between 30 and 100 minutes. When Fe_2O_3 particles are present, the outlet concentration quickly increases, peaking at 32% after 45 minutes. The CO from char gasification is being oxidized by the iron particles producing more CO_2. After 100 minutes, the concentration is down below 24% CO_2 and therefore much closer to the inlet concentration. Hence, the reaction is much closer to completion compared to the experiment in the absence of any metal oxide. The large increase in CO_2 concentration due to the Fe_2O_3 means more CO_2 is available to gasify the char and by Le Chatelier's Principle, increases the rate of char gasification.

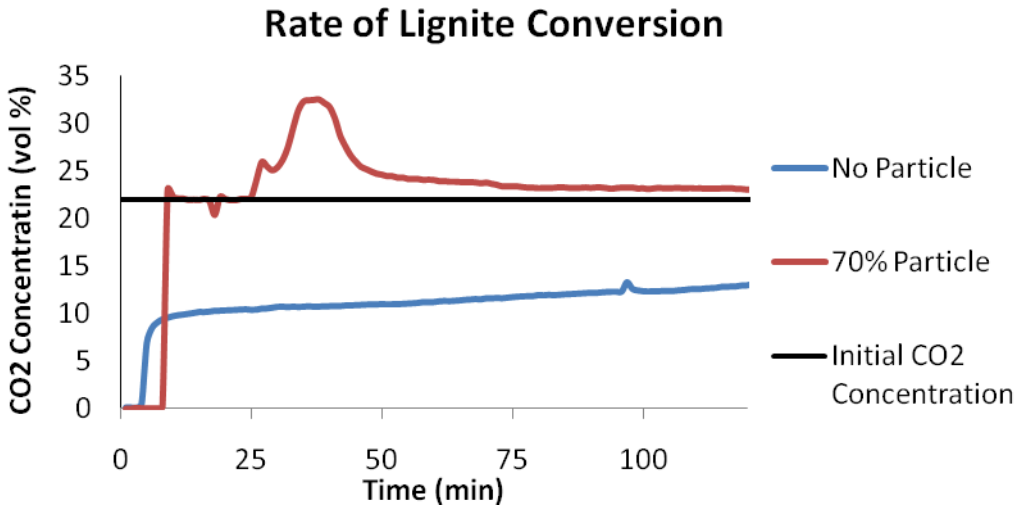

Figure 16: Influence of Fe_2O_3 particles on rate of lignite char gasification.

Fluidization

From altering the F:P ratio during coal fluidization, it was found that the ratio did not have a significant effect on U_{mf}. For each ratio, the U_{mf} was about 5-7 cm/s, signified by the large drops in ΔP in Figure 17 below. At these points, fluidization was observed. When sand was fluidized without iron particles, the U_{mf} was higher. The void space of the iron particles effectively increases the gas velocity inside the fluidizer. This results in the sand having a lower U_{mf} when particles are present. However, as long as iron particles are present in the fluidizer, there is no distinguishable relationship between F:P ratio and U_{mf}. Therefore, any weak dependence on gas velocity is negligible and the final F:P ratio will be decided by the kinetics of char gasification and iron reduction.

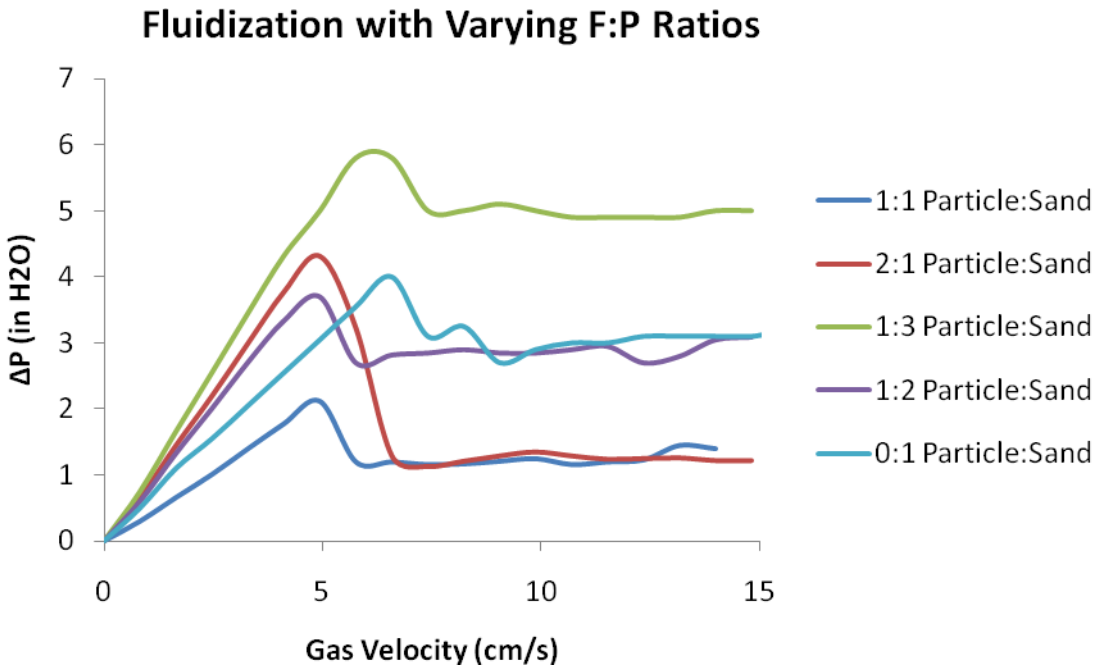

Figure 17: Comparison of U_{mf} for varying F:P ratios using sand to simulate coal.

Fluidization of the large grain wood biomass without any inert to enhance the fluidization was unsuccessful under the conditions tested. Figure 18 below shows the ΔP across the fluidizer and the bed height as the gas velocity was increased. The bed height continued to increase with pressure drop as the gas velocity was increased. Though the gas velocity was high, the elevated void fraction of the large grain wood biomass kept the ΔP low. The high void fraction in conjunction with holes that formed through the biomass where the gas could escape prevented fluidization. The marker in Figure 18 indicates where the biomass began to entrain out of the top of the fluidizer. Since the gas velocity was so high at that point, small particles of biomass adjacent to the gas escape began to become entrained.

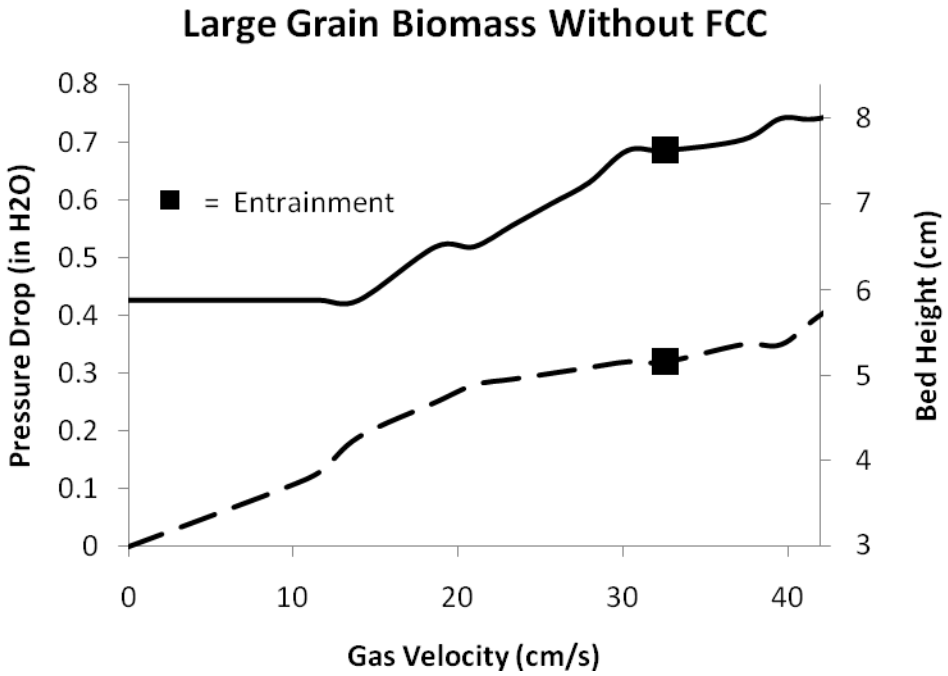

Figure 18: Biomass fluidization without any FCC added. The dashed lines indicates pressure differential across the fluidizer while the solid line indicates bed height.

Addition of FCC aided in breaking apart the biomass bonds between grains and in reducing the void fraction. However, a high percentage of FCC was required to fluidize the biomass. An FCC mass of at least 80% of the total mass of the wood was required for fluidization. Above 105%, the total mass inside the fluidizer became too high and the gas velocity needed to be increased beyond practical levels. Figure 19 below shows that although there were points of substantial drops in ΔP, they did not signify fluidization. These points were typically associated with formations of bubbles or large voids within the bed, allowing the gas to escape past the bed of biomass. Points of significant drop in ΔP after bubble formation indicated partial or temporary fluidization. In these cases, only a fraction of the biomass would fluidize while the rest remained stationary. Typically, the partial fluidization only lasted 4-8 seconds before

collapsing or forming a hole in the bed. Both bubble formation and partial fluidization resulted in an increase in bed height which was expected. However, when the biomass did fluidize, there was no associated drop in ΔP. This is likely due to the complexity of fluidizing two different sized, non-ideal particles with a third stationary and much larger particle.

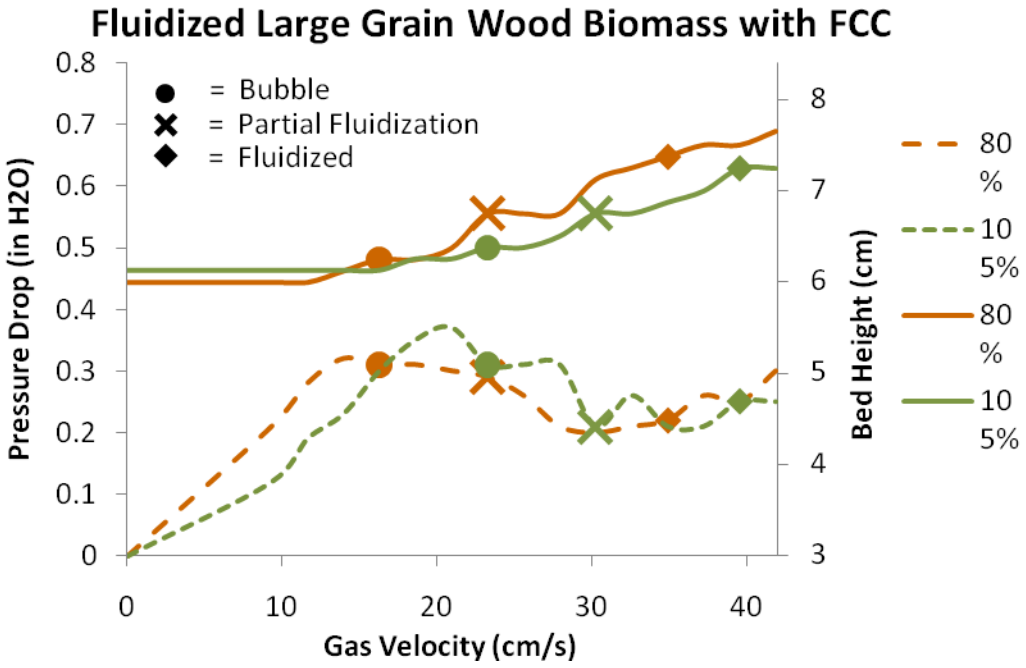

Figure 5: Large grain wood biomass fluidization with 80% and 105% FCC by mass of wood. Dashed lines are pressure differential across the fluidizer while solid lines are height of the biomass/FCC/iron particle bed.

The smaller grain wood was also unable to be fluidized without the addition of FCC. There is a significant drop in ΔP shown in Figure 20 below, however, similar to the larger grain wood, this is not indicative of fluidization. Since wood has the capacity to agglomerate, the smaller grain wood can form structure and hold together. When enough

pressure builds up, a bubble forms and gas escapes through the bed. In a more typical packed bed, the bubble collapses back in on itself. However, in the case of the small grain wood, the bubble moves through the wood particles, forms a structure and a hole remains where the bubble came through. The opening allows the gas through, dropping the ΔP, and preventing fluidization. A large amount of particles adjacent to the gap tended to become entrained out of the fluidizer as well.

Addition of FCC successfully stopped the agglomeration of the wood particles. In cases with low percentages of FCC by mass, fluidization occurred at low gas velocities but was not stable; the wood fluidized for up to 20 seconds before giving way to structural holes and fluidization was lost. Wood grains separated from the FCC and continued to be entrained out of the fluidizer. The wood grains are not dense relative to the FCC, so where the gas velocity was not high enough to entrain the FCC, it did entrain the wood particles. However, as percentage of FCC increased, fluidization stability increased and entrainment decreased. Once the amount of FCC reached 90% of the wood grain mass, fluidization was completely stable with almost no entrainment. At this point, an interesting effect was observed. As is shown below in Figure 21, at the point of fluidization, ΔP increased rather than decreased. The openings that formed before fluidization kept the ΔP low. When fluidization was achieved and gaps were destroyed, gas could not escape as easily, increasing the ΔP. The increase in ΔP helps to explain the instability of fluidization for the tests with lower quantities of FCC as well.

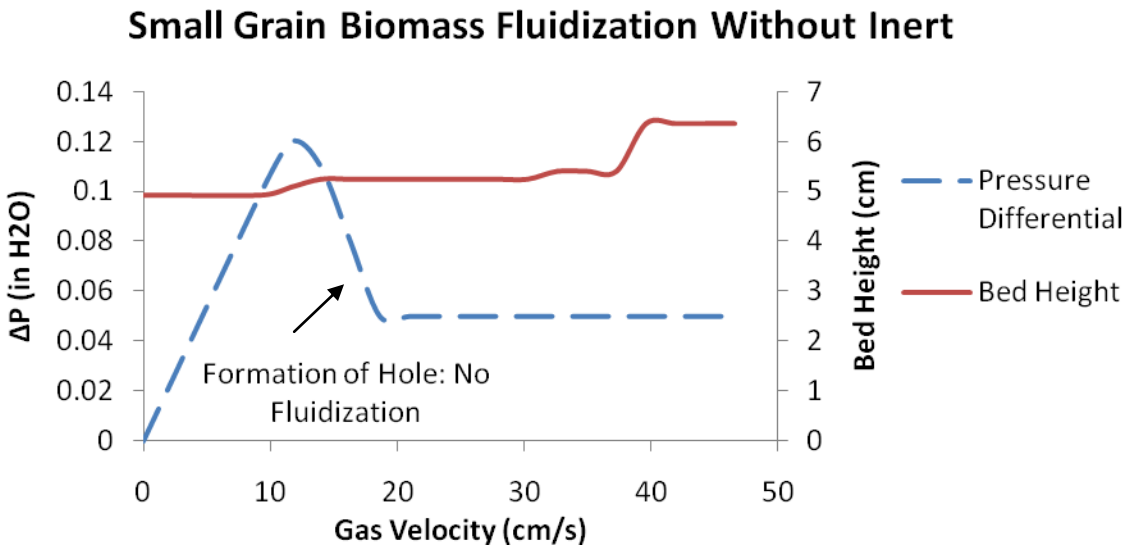

Figure 20: Small grain biomass fluidization without FCC inert particles. The dashed line represents pressure differential across fluidizer and the solid line is the bed height.

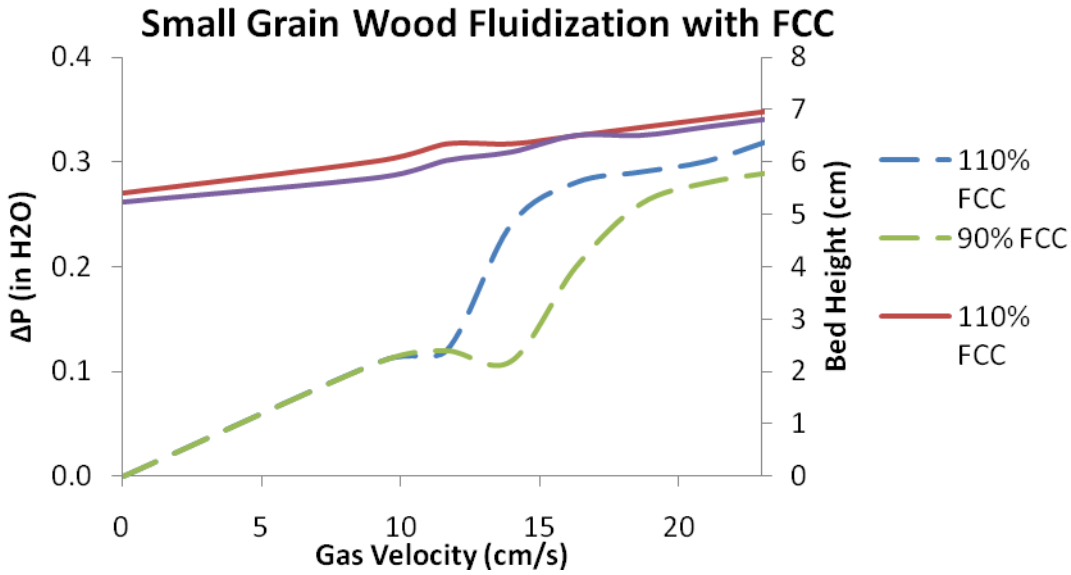

Figure 21: Fluidization of small grain wood biomass with 90% and 110% FCC, the region in which fluidization was stable. Dashed lines indicate pressure differential while solid lines mark bed height.

Both size grains of wood biomass require nearly 100% FCC by mass to achieve fluidization. While the smaller grain wood biomass has U_{mf} of 12-15 cm/s, which is

slightly higher than coal, the larger grain wood biomass requires 35-40 cm/s. A gas velocity this high would not be economical when compared with coal and therefore would not be supported in the commercial realm. However, the U_{mf} of the smaller grain wood biomass is still within the same order of magnitude as the U_{mf} of coal. The fine grain wood is therefore a possible candidate for coal replacement in the CDCL process.

Cold Model: Particle Outflow

In all cases, the bottom air injection led to a higher flow rate of particle than top air injection. This was expected, because the air flow from the bottom orientation is more in line with direction of the exiting flow stream, helping to push the particle out of the pipe. After three tests with the 1.5" pipe diameter, it was clear that the smaller diameter would require the same air injection flow rate to achieve similar particle flow rates. Therefore, most tests were conducted using the 2" pipe diameter. For comparison of pipe angle, it was clear that a smoother angle gave significantly higher particle flow rates. This was also predicted, since the smoother angle would provide for a more gradual change in momentum of the particle, as well as a better path for the air injection to take towards to exit of the pipe. Furthermore, a smoother angle provides for less resistance as the particle exits the pipe. Concerning blade size, the experiments showed that the smaller blade also gave rise to higher particle flow rates, since it provides less resistance. Model 7, the configuration with a sharp angle, the larger blade, and top air injection, did not provide any particle flow because this combination has the highest resistance. Model 1 was eventually adopted because it provided for a relatively low but controlled flow rate, both qualities which were desired in the final design. However, after further use of Model 1,

another air injection was placed instead of the blade on the bottom of the pipe directing air straight up. Since the air flow rate could be controlled, it provided better management over particle flow, and fewer instances of particle holdup in the pipe.

Conclusions and Recommendations

The method of using CO_2 to gasify coal char to increase the char conversion rate has proven to be effective. Lignite char oxidation was 3.6% higher when 5% CO_2 and air were contacted with the char compared to oxidation with air alone. For the two chars tested, lignite and sub-bituminous char, the presence of CO_2 improved conversion by reaction with Fe_2O_3 in a given time by a factor of two in the TGA compared to an inert environment. In the fixed bed, which is a more accurate simulation of the CDCL design, char conversion was increased 5-11 times by the gasification enhancer CO_2. It has been shown that the presence of CO_2 significantly enhances the gasification and conversion of coal char, regardless of coal type.

The oxygen carrier particles have a significant effect on char conversion. It was found that ideal mixtures of Fe_2O_3 and char increased char conversion in CO_2 two times for lignite, and five times for sub-bituminous char compared to pure char. Furthermore, GC analysis of the fixed bed experiments shows that the presence of Fe_2O_3 is the key to increasing the rate of char conversion when CO_2 is present.

Fluidization of the coal char is crucial to maintaining high char conversion. It was found that fluidization of the coal-simulating sand was not dependent on the relative amount of particles in the fluidizer. This is important because it means the amount of particles in the reactor and their residence time will be determined by the kinetics and not the fluidization of the char.

In assessing the potential of wood biomass as a coal replacement in the CDCL process, it was determined that at least 80% of the FCC inert particle was required to fluidize either size of wood biomass. Large grain biomass is not a suitable choice due to

its U_{mf} being about six times greater than sand. However, the U_{mf} of the small grain wood biomass was about twice as large as that for sand, and therefore within the realm of feasibility. In the future, other inert particles should be examined to see if it might be possible to lower the U_{mf} as well as the total amount of inert required to fluidize the small grain wood biomass. Furthermore, the kinetics of biomass gasification with CO_2 and reaction with Fe_2O_3 must be studied in depth to further determine feasibility.

To transfer particles from the moving bed of the reducer to the combustion train, a high resistance design was found to be most controllable and reliable. A 2" pipe was used with a sharp pipe angle, top gas injection, and 1/3 blade which was later replaced with a second gas injection due to its better controllability. This design has proven reliable in subsequent tests, providing the desired management over particle flow out of the reducer and into the combustion train. Further examination of the cold model should explore dynamics of particle entrainment in the combustor, design of the cyclone at the top of the reducer, and the pressure profile of the reducer, all of which are important factors to the CDCL process design.

This study has shown that the CDCL process is an effective technology and promises to help in mitigating global climate issues while also having the capacity to meet growing energy demands. The results show that CDCL is well on its way to fulfilling that promise. Addressing the issue of climate change requires swift action and through a retrofit design, CDCL can do just that. This novel process may very well become a vital technology for the energy of tomorrow.

Notation

AR4	IPCC Fourth Assessment Report
C	Carbon/Char
CDCL	Coal Direct Chemical Looping
CO	Carbon Monoxide
CO_2	Carbon Dioxide
DACC	Detection and Attribution of Climate Change Report
EIA	US Energy Information Administration
FCC	Fluidized Catalytic Cracking Particle
F:P	Fuel to Particle Ratio
Fe	Iron
FeO	Iron (II) Oxide
Fe_2O_3	Iron (III) Oxide
G	Percent char gasified in fixed bed
GC	Gas Chromatography
GHG	Greenhouse Gases
He	Helium
IGCC	Integrated Gasification Combined Cycle
IPCC	Intergovernmental Panel on Climate Change
kWh	Kilowatt hours
kW_{th}	Kilowatts thermal
m	Original mass of char in fixed bed (g)
N_2	Nitrogen
ΔP	Differential Pressure (inches of H_2O)
PCC	Pulverized Coal Combustion
U_{mf}	Minimum Fluidization Velocity (cm/s)
X	Original mass of iron in fixed bed (g)
y	Percent mass gained by iron in TGA

Bibliography

1. IPCC 2007:. *Climate Change 2007: Synthesis Report. Contribution of Working Groups I, II, and III to the Fourth Assessment Report of the Intergovernmental Panel on Climate Change.* [Core Writing Team, Pachauri, R.K and Reisinger, A. (eds.)] : s.n., IPCC, Geneva, Switzerland.

2. Past Climate Change. *Climate Change Science.* [Online] U.S. Environmental Protection Agency, September 28, 2009. [Cited: April 22, 2010.] http://www.epa.gov/climatechange/science/pastcc.html.

3. **Stott, Peter A., et al.** Detection and Attribution of Climate Change: A Regional Perspective. *Wiley Interdisciplinary Reviews: Climate Change.* March 5, 2010, pp. 192-211.

4. *Annual Energy Review 2008.* Washington, D.C. : U.S. Department of Energy: Energy Information Administration, June 2009.

5. Sciene: Atmospheric Changes. *US Environmental Protection Agency: Climate Change.* [Online] November 5, 2009. [Cited: April 28 2010, 2010.] http://www.epa.gov/climatechange/science/recentac.html.

6. **Boden, T.A., G. Marland, R.J. Andres.** *Global, Regional, and National Fossil-Fuel CO2 Emissions.* Oak Ridge, Tenn. : Carbon Dioxide Information Analysis Center, Oak Ridge National Laboratory, U.S. Department of Energy, 2009.

7. Global Warming. *Union of Concerned Scientists: Citizens and Scientists for Environmental Solutions.* [Online] 2010. [Cited: May 1, 2010.] http://www.ucsusa.org/global_warming/science_and_impacts/science/each-countrys-share-of-co2.html.

8. *Inventory of U.S. Greenhouse Gas Emissions and Sinks: 1990-2008.* Washington, DC : U.S. Environmental Protection Agency, April 15, 2010.

9. International Electricity Generation. *U.S. Energy Information Administration.* [Online] U.S. Department of Energy, December 8, 2008. [Cited: April 10, 2010.] http://www.eia.doe.gov/emeu/international/electricitygeneration.html.

10. International Energy Outlook 2009: Highlights Section. *U.S. Energy Information Administration.* [Online] U.S. Department of Energy, May 2009. [Cited: April 10, 2010.] http://www.eia.doe.gov/oiaf/ieo/highlights.html.

11. **Ram C. Sekar, John E. Parsons, Howard J. Herzog, and Henry D. Jacoby.** *Future Carbon Regulations and Current Investments in Alternative Coal-Fired Power Plant Designs.* s.l. : MIT Joint Program on the Sciene and Policy of Global Change, December 2005.

12. *Carbon Sequestration Technology - Current Status and Future Outlook.* **Sasaki, Koichi.** s.l. : Institute of Energy Economic, Japan, November 2003.

13. **Xiaochun Xu, Chunshan Song, Ronald Wincek, John M. Andresen, Bruce G. Miller, and Alan W. Scaroni.** *Separation of CO2 from Power Plant Flue Gas Using Novel CO2 "Molecular Basket" Adsorbent.* University Park, PA : Clean Fuels and Catalysis Program, The Energy Institute, and Department of Energy & Geo-Environmental Engineering, The Pennsylvania State University, 2003.

14. **Xiaonian Li, Edward Hagaman, Costas Tsouris, and James W. Lee.** *Removal of Carbon Dioxide from Flue Gas by Ammonia Carbonation in the Gas Phase.* Ridge, Tenn. : American Chemical Society, 2003.

15. *Integrating MEA Regeneration with CO2 Compression to Reduce CO2 Capture Costs.* **Kevin S. Fisher, Carrie Beitler, Curtis Searcy.** Buda, TX : U.S. Department of Energy, National Energy Laboratory, Pittsburgh PA, Fourth Annual Conference On Carbon Capture and Sequestration DOE/NETL, May 2-5, 2005.

16. *The Economics of CO2 Capture.* **Herzog, Howard J.** Interlaken, Switzerland : Massachusetts Institute of Technology (MIT) Energy Laboratory, Fourth International Conference on Greenhouse Gas Control Technologies, August 30 - September 2, 1998.

17. *Syngas Redox Process to Produce Hydrogen from Coal Derived Syngas.* **Puneet Gupta, Luis G. Velazquez-Vargas, and Liang-Shih Fan.** Columbus : Energy & Fuels, 2007, Vol. 21.

18. *The Reduction of Iron Oxides by Volatiles in a Rotary Hearth Furnace Process: Part II. Reductin of Iron Oxide/Carbon Composites.* **I. Sohn, R.J. Fruehan.** s.l. : Metallurgical and Material Transactions B, 2006, Vol. 37B.

19. *Project Fact Sheet: Coal Direct Chemical Looping Retrofit to Pulverized Coal Power Plants for In-Situ CO2 Capture.* s.l. : U.S. Department of Energy, Office of Fossil Energy, 2009.

20. Pulverized Coal Power. *World Resources Institute.* [Online] [Cited: May 1, 2010.] http://www.wri.org/publication/content/10338.

21. *Fluidization of Biomass Particles: A Review of Experimental Multiphase Flow Aspects.* **Heping Cui, John R. Grace.** Vancouver, Canada : Chemical Engineering Science, 2006, Vol. 62.

22. Coal & Its Uses - Coal Classification. *Australian Coal Association.* [Online] 2008. [Cited: May 1, 2010.] http://www.australiancoal.com.au/coal-and-its-uses_coal-classification.aspx.

Appendix A

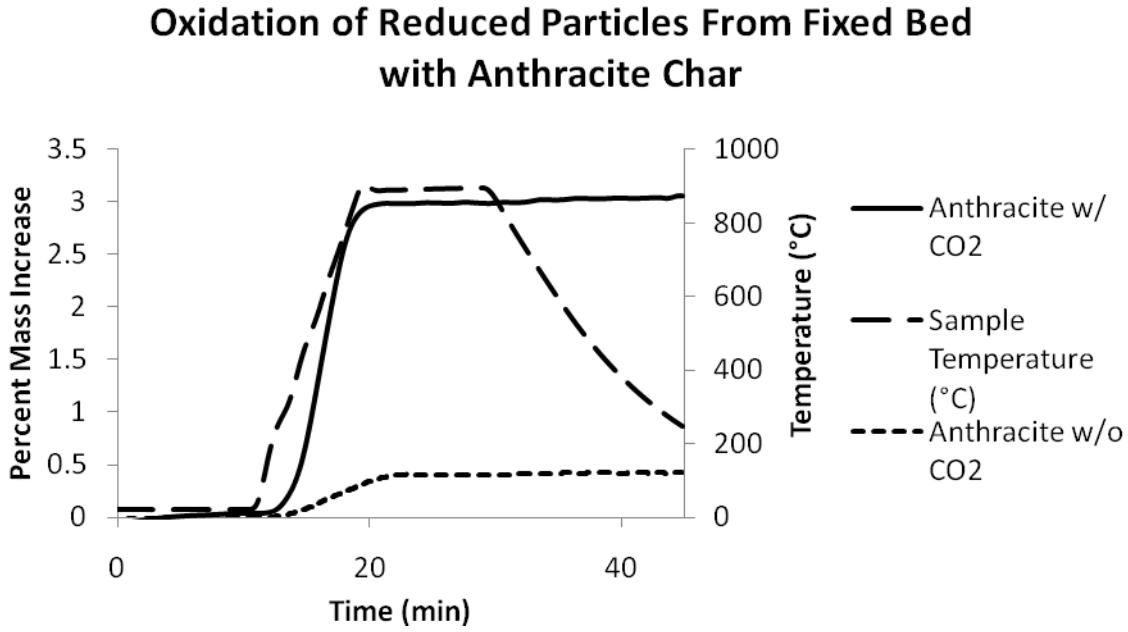
Oxidation of Reduced Particles From Fixed Bed with Anthracite Char
Percent Mass Increase
3.5
3
2.5
2
1.5
1
0.5
0
0
20
40
Time (min)
1000
800
600
400
200
0
Temperature (°C)
Anthracite w/ CO2
Sample Temperature (°C)
Anthracite w/o CO2

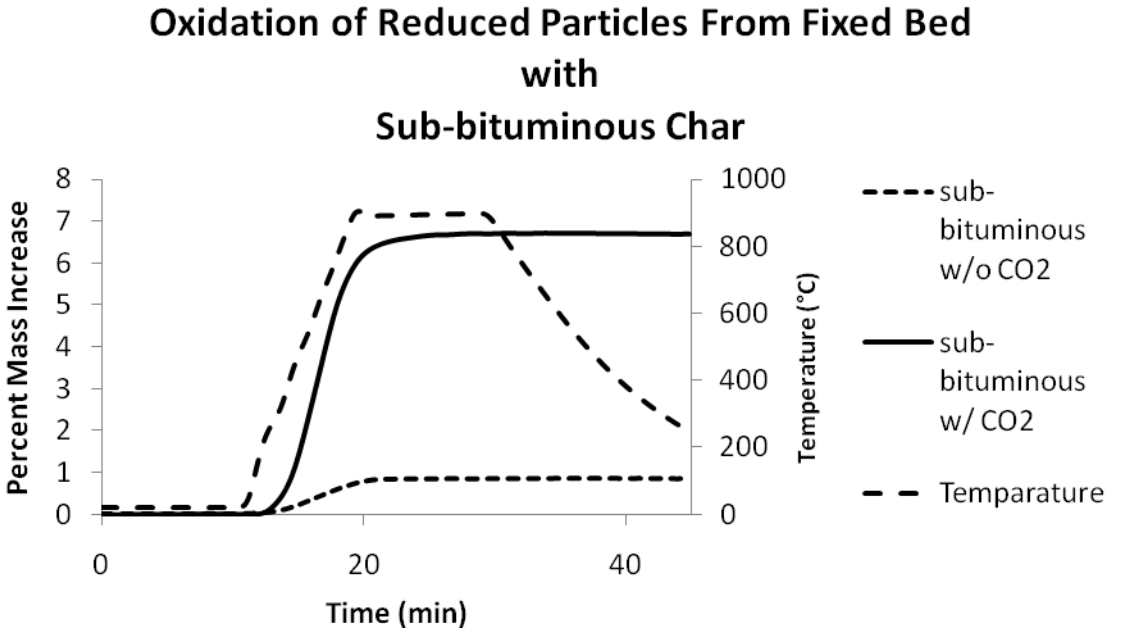
Oxidation of Reduced Particles From Fixed Bed with Sub-bituminous Char
Percent Mass Increase
8
7
6
5
4
3
2
1
0
0
20
40
Time (min)
1000
800
600
400
200
0
Temperature (°C)
sub-bituminous w/o CO2
sub-bituminous w/ CO2
Temparature

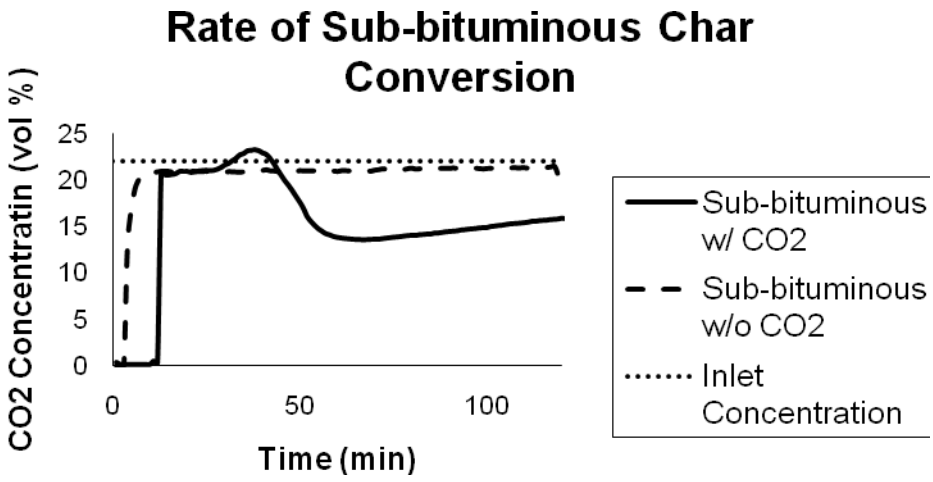

Reducer-Combustor Transition Design Results

Model #	Pipe Size (")	Angle Shape	Blade Enclosure	Air Injection	Avg Flow Rate (kg/min)
1	2	Sharp	1/3 Blade	Top Air	3.9
2	2	Smooth	1/3 Blade	Top Air	5.0
3	2	Sharp	1/3 Blade	Bottom Air	5.4
4	2	Smooth	1/3 Blade	Bottom Air	12.9
5	2	Smooth	1/2 Blade	Bottom Air	5.3
6	2	Smooth	1/2 Blade	Top Air	3.3
7	2	Sharp	1/2 Blade	Top Air	0.0
8	1.5	Sharp	NO	Bottom Air	24.1
9	1.5	Sharp	NO	Top Air	7.2